
ASSESSMENT OF FREQUENCY CONVERSION EFFICIENCY INSIDE A MICROCAVITY

E.W. Likta, N. Yakubu and S. M. Kabir

Department of Physics,
University of Maiduguri, Maiduguri, Borno State. Nigeria.
E-mail Address: emmalikta2014@gmail.com

ABSTRACT

It is known that optical microcavities have two surface structures. There are two kinds of microcavity: stationary and travelling wave cavity. Optical cavity is also known as an arrangement of mirrors or other optical components that creates a cavity resonator for light waves. There are many reflections of light from the cavity that show in modes; the modes are divided into two types, these are transverse and longitudinal modes. The goal of this paper focuses on when the microcavity's refractive index is changed, converting light intensity, frequency, and the frequency converted light intensity. The method used is the 1D structure cavity theoretically. The results were obtained; also it was observed that the microcavity refractive index was changed. The frequency converted light intensity was obtained.

Keywords: *Microcavity, Stationary wave, Travelling wave, Transverse modes and Longitudinal modes*

INTRODUCTION

An optical micro cavity or micro resonator is a structure made of two surfaces that reflect light, such as a spacer layer or optical medium, or a wave guide that has been wrapped in a circle to create a ring (Vahala, 2003). A stationary wave cavity is the first kind, while a travelling wave cavity is the second. Because it is sometimes just a few micrometers thick, with the spacer layer perhaps even being in the nanometer range, it is known as a micro cavity (Kippenberg et al., 2007). This creates an optical cavity or resonator, just like in conventional lasers, allowing a standing wave to develop inside the spacer layer or a traveling wave to circle the ring (Savchenkov et al., 2007). An arrangement of mirrors or other optical components that creates a cavity resonator for light waves is known as an optical cavity, resonating cavity, or optical resonator (Ji et al., 2017). The gain medium is surrounded by optical cavities, which also serve to provide feedback for the laser light. They are also utilized in some interferometers

and optical parametric oscillators (Emire et al., 2016). The many reflections of light contained in the cavity result in modes with particular resonance frequencies. The two types of modes are transverse modes, which have distinct intensity patterns across the cross-section of the beam, and longitudinal modes, which differ solely in frequency (Aspelmeyer et al., 2012). A cavity resonator is a mechanical device that reverberates in a hollow interior area. In microwave transmitters, receivers, and test equipment, microwave cavities made of hollow metal boxes are utilized instead of tuned circuits, which are employed at lower frequencies, in electronics and radio. Helmholtz resonators are acoustic cavity resonators, in which sound is generated by air vibrating in a cavity with a single aperture (Aspelmeyer et al., 2014).

MATERIALS AND METHODS

As illustrated in Figure 1, the cavity used in this investigation is a 1D structure made up of alternating Bragg layers. The high-index material's refractive index is chosen to be $n_1 = 3.51$ and the low-index material's refractive index to be $n_2 = 2.95$. These values correspond to typical values for GaAs and AlAs at telecom wavelengths, respectively. For layers with indices n_1 and n_2 , the thickness of quarter layers is set to 91.9 nm and 108.0 nm, respectively. There are 19 pairs of bottom mirrors and 7 pairs of top mirrors around the layer with a thickness of 363.87 nm. The cavity's asymmetrical form permits more loss of it boosts output from the front mirror and light from the front mirror. Air layers with a 1- μ m thickness are positioned before and after the cavity, as seen in Figure 1. The aforementioned configurations result in a cavity with a quality factor of $Q = 424$, which translates to a storage time of $\tau_{cav} = 288$ fs at a resonance frequency of $\omega = 7807$ cm⁻¹.

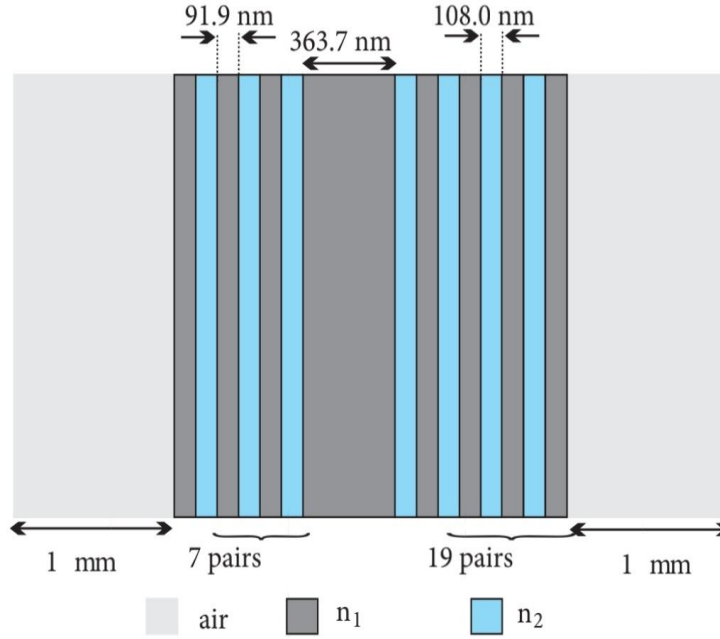


Figure 1. The structure of the cavity and the surrounding media.

The λ -layer with a thickness of 363.7 nm is sandwiched between 7 and 19 pairs of alternating quarter layers at the top and at the bottom. The thickness of the air layer before and after the structure is 1 μm .

The time resolved reflected spectra from the microcavity are calculated using the model detailed by (Yüce, 2016). For this reason, here I provide the necessary steps in our model. An electric field is launched at the structure at $t_0 = 0$ with a form given in Eq. (1).

$$E(z_0 t) = E_0(z_0) e^{-i\omega t} e^{\left(\frac{t-t_0}{t}\right)} \quad 1$$

where E_0 is the incoming field's amplitude, the angle's frequency, t , the time, z , and the length of the Gaussian pulse's launch at t_0 . The structure's refractive index of the n_1 layers is programmed to change over time while the index of the n_2 layers and the air layers remains constant throughout the computation (Fürst et al., 2010). Because of this, the electric field is re-expressed as Eq. (2) when the field is inside the n_1 layers.

$$E(z_i - t) = E_0(z_0) e^{-i\omega(n(t)\frac{z-z_0}{c})} \left(c^{-\left(n(t)\frac{z-z_0}{c}\right)\frac{t_0}{c}} \right) \quad 2$$

The Fresnel coefficients are produced when the electric field impinges on a contact; some of the electric field is transmitted and some of it is reflected. Here, the reflected and transmitted ratios—which determine the strength of the forward and backward propagating electric fields at a certain location are calculated using the Fresnel coefficients. As a result, the electric field at point z is described by Eq. (3) as the sum (E_{sum}) of the electric fields that propagate forward and backward.

$$E_{sum} = E^f(Z_o, n(Z, t) \cdot \frac{(Z-Z_o)}{c}) \cdot t + E^b(Z_o, n(z, t) \cdot \frac{(Z-Z_o)}{c}) \cdot r \quad 3$$

where E^f is the magnitude of the forward propagating field, and E^b is the magnitude of the backward propagating field, and t and r are the Fresnel reflection and transmission coefficients from the pertinent interfaces. Eq. (4) is used to determine the resulting spectrum at a specific point.

$$E_{sum}(Z, W)^2 = \sum_o^t E_{sum}(z, t) \cdot e^{-(i2\pi w \delta t)} \quad 4$$

Results and Discussion

The results obtained are as follows:

Table 1: Reflection Spectra for Microcavity

frequency	switched	Unswitched
7300	0.99	0.99
7400	0.99	0.99
7500	0.99	0.99
7600	1	0.99
7700	0.99	0.99
7800	0.85	0.88
7850	1.04	0.99
7900	0.98	0.99
8000	0.98	0.99
8100	0.99	0.99
8200	0.99	0.99
8300	0.99	0.99

Table 2: Resonance Frequency for the Microcavity

Delay	Frequency
-3	7807.2
-2.9	7807.2
-2.8	7807.2
-2.7	7807.2
-2.6	7807.2
-2.5	7807.2
-2.4	7807.2
-2.3	7807.2
-2.2	7807.2
-2.1	7807.8
-2	7807.8
-1.9	7807.8
-1.8	7807.8
-1.7	7807.8
-1.6	7807.8
-1.5	7807.8
-1.4	7807.8
-1.3	7808.2

-1.2	7808.2
-1.1	7808.2
-1	7808.8
-0.9	7807.8
-0.8	7807.2
-0.7	7807.2
-0.6	7806.9
-0.5	7806.1
-0.4	7805.5
-0.3	7804.6
-0.2	7803
-0.1	7802.2
0	7804
0.1	7806.9
0.2	7806.9
0.3	7806.9
0.4	7806.9
0.5	7806.9
0.6	7806.9
0.7	7806.9
0.8	7806.9
0.9	7806.9
1	7806.9

Table 3: Integrated Intensity Color for a function of Pump Power

pump power	color intensity
10	30
20	60
30	100
40	120
50	150
60	180
70	200
80	220
90	240
100	260

110	280
120	300
130	325
140	350
150	375
160	400
170	425
180	450
190	475
200	500

Table 4: Integrated Intensity Color for a Function of Pump Pulse.

Pump Duration	Colour Intensity
0	170
50	300
100	450
150	550
200	570
250	575
300	570
350	555
400	550
450	530
500	520
550	500
600	490
650	475
700	460
750	440
800	420
850	410
900	400

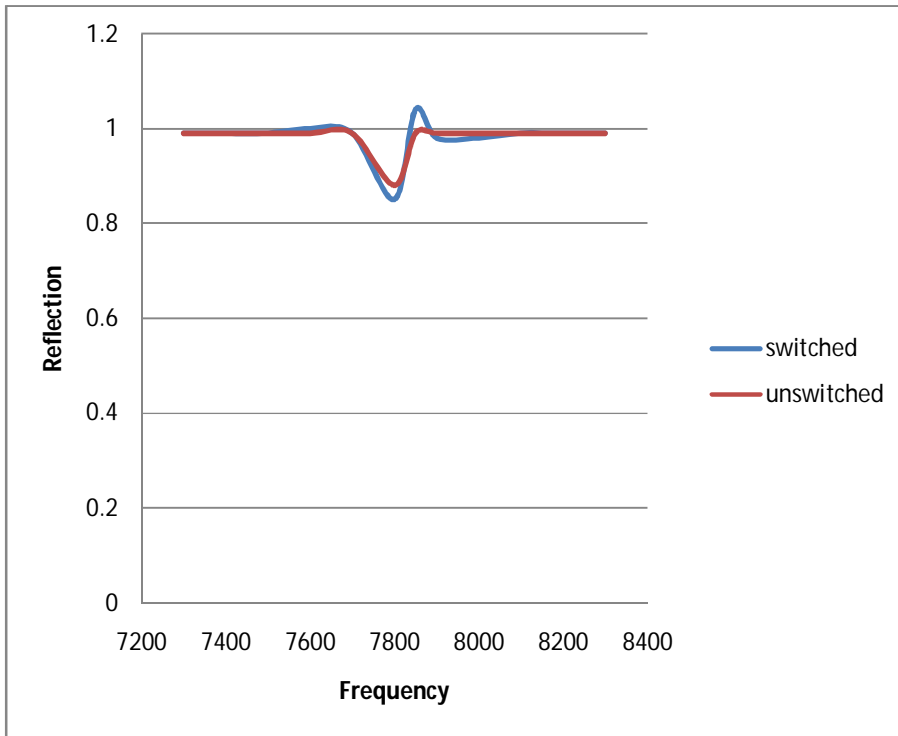


Fig 2: Frequency against Reflection for Micro cavity

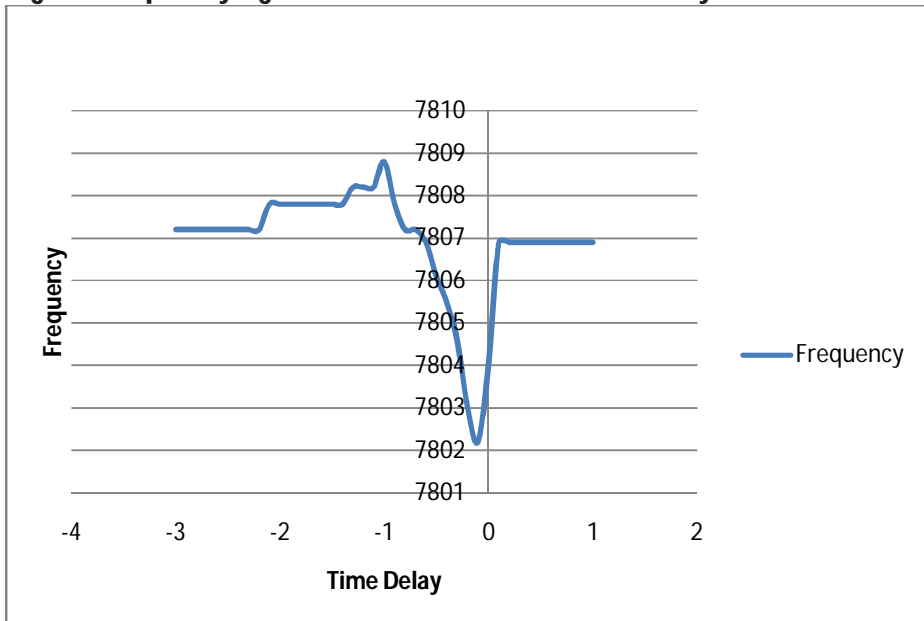


Fig 3: Frequency against Time delay for Microcavity

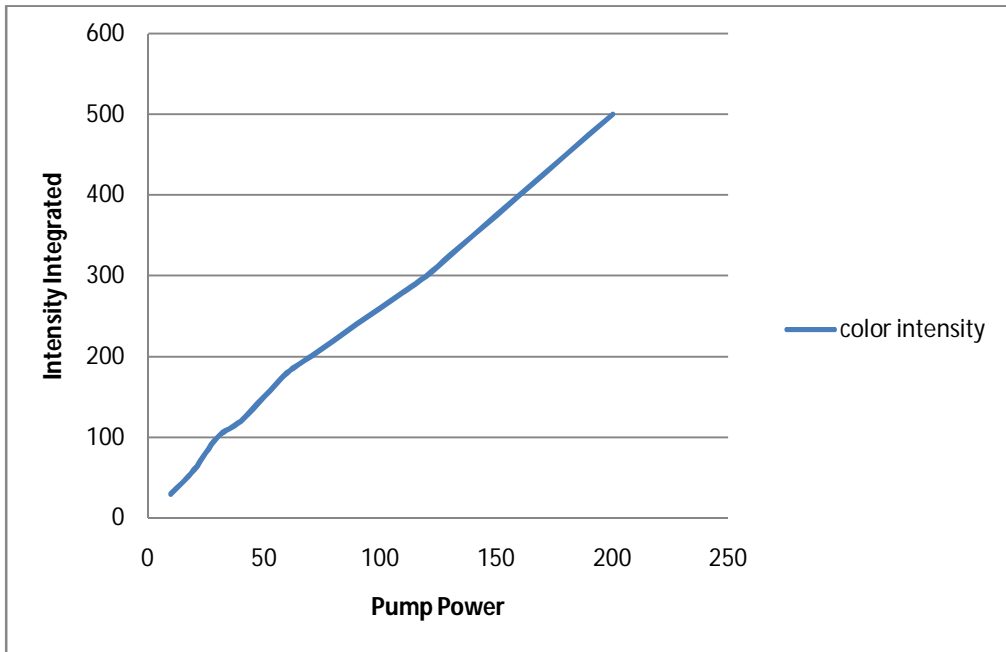


Fig 4: Intensity integrated against Pump power for Microcavity

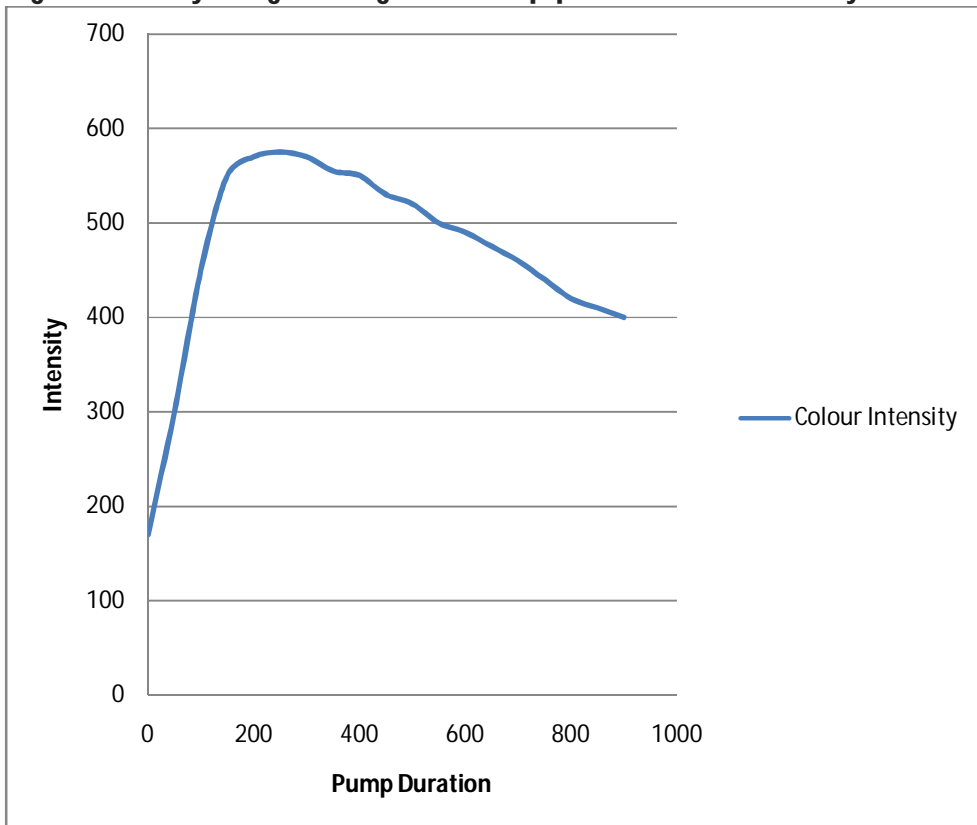


Fig 5: Intensity against Pump Duration for Microcavity

DISCUSSION

Utilizing the configuration, the unswitched reflection spectra from the cavity structure are determined. given in figure 2 and the result is provided in figure 3. As can be seen in figure 3, the resonance frequency of the unperturbed cavity is centered at $\omega_{res} = 7807.0cm^{-1}$ ($\gamma_{res} = 1280.9$ mm). The reflectivity at the stop band is 0.999 and is flat within the frequency range provided in figure 2.

Through the use of an ultra-short pulse with duration of just $\tau = 100fs$, the cavity's refractive index may be changed. The relation $n = n_i + n_{il} \cdot I_{pu}$ is used to predict that the refractive index of the n_i layers will rise linearly where I_{pu} is the intensity of the switch pulse (pump pulse), n_i is the unperturbed refractive index, and n_{ni} is the nonlinear index coefficient. The electronic Kerr effect is characterized by the immediate switching of the cavity refractive index. The nonlinear index coefficient is assumed to be $n_2 = 1.5 \times 10^{-5} \text{ cm}^2/\text{GW}$ and for the switching spectra shown in figure 2, the pump pulse's intensity is set at $I_{pu} = 162 \text{ GW}/\text{cm}^2$.

Due to the higher refractive index, the cavity's resonance frequency in figure 3 moves to a lower frequency ($\omega' = 7802.3cm^{-1}$). Resonance frequency variation ($\omega = 4.7 \text{ cm}^{-1}$) translates into an index variation of $n = 0.06\%$. The phase of light within the cavity quickly changes due to a quick index shift within 100 fs, which causes a change in frequency as shown by Eq. (5). It is evident from Eq. (5) that the frequency conversion of light is caused by the rate of phase change ($\dot{\phi}$). It should be noted that the phase change is inversely correlated with the refractive index change $\partial n(5)$.

$$\partial n(t) = \frac{\partial \phi}{\partial t} \tag{5}$$

The switching spectra shown in figure 3 can be used to observe the frequency conversion of light. When a structure is switched, the reflectivity rises above unity, indicating the presence of previously undiscovered frequencies inside the cavity. Although it might not be conclusive, the additional light that is more than unity is a strong indicator of frequency converted light. It provides several reliable standards for figuring out light's frequency conversion below. From the switch spectra, it

can be inferred that the intensity has changed between frequencies, increasing at frequencies higher than the cavity resonance and decreasing at frequencies lower than the cavity resonance.

After that, it encourages a pump/probe method in my computations to provide time-resolved spectra at various times. Figure 4 plots the cavity's resonance frequency as a function of the interval between the pump pulse (also known as the switch pulse) and the probe pulse. In figure 4, the pump and probe signals reach the cavity simultaneously with zero delay. As seen in figure 4, the change in the cavity refractive index occurs within 1 ps. Given the storage of the probe field in the cavity, the cavity resonance returns to the unswitched resonance at longer time scales despite the pump pulse having a length of $T_{pu} = 100$ fs to the $T_{cav} = 288$ fs, to be precise. Pump pulses come before probe pulses at positive time delays, whereas probe pulses arrive before pump pulses at negative time delays and the refractive index of the probe field inside the cavity increases or decreases depending on when the pump pulse arrives. Due to this, the rate of phase change will be positive and negative, causing blue- and red-shifted light, respectively. The integrated color converted light intensity is shown against pump power in Figure 4. When can be observed in Eq. (5), when the pump intensity increases, the rate at which the refractive index changes also increases, leading to an increase in frequency shift. The outcomes are consistent with earlier hypotheses and findings. The integrated color converted light intensity is shown against pump pulse time in Figure 4. As can be seen, the total amount of color-converted light grows up to 260 fs before beginning to decline beyond that. The overall intensity of the frequency converted light does not rise even if the rate of phase change accelerates with shorter pump pulse length. Figure 5 shows that the pump pulse duration must match the cavity storage time ($T_{cav} = 288$ fs) in order to provide the greatest quantity of color transformed light. We can draw the conclusion that color conversion in a microcavity behaves differently than it does in an open medium.

The frequency converted light intensity within a microcavity increases with an increasing rate of change of the microcavity's refractive index, according to studies that concentrate on nonlinear frequency conversion of light inside a microcavity. More significantly, this research demonstrates that when the index perturbation's length is matched to the

cavity storage period, the intensity of the frequency converted light is maximized. The findings offer the best settings for modifying the color of light inside a microcavity, a goal pursued for optical communication technologies on chips. In quantum optics, cavities are commonly used as profound structures for regulating quantum light sources. The findings will resoundingly back fundamental investigations into cavity-based single photon frequency control.

REFERENCE

- Aspelmeyer M.; Meystre P.; Schwab, K. (2012): Quantum Optomechanics. Publisher Physics Today. **65** (7): 29–35.
- Aspelmeyer M; Kippenberg T J.; Marquardt F (2014): Cavity optomechanics. Reviews of Modern Physics. **86** (4): 1391–1452.
- Emre Y, Georgios C, Julien C, Jean M.G, Willem L.V (2016): Optimal all-optical Switching of a micro cavity Resonance in the telecomm range using the electronic Kerr effect. Publisher Journal of Optics Express, Vol.24 page 239-252
- Fürst, J. U.; Strelakov, D. V.; Elser, D.; Aiello, A.; Andersen, U. L.; Marquardt, Ch.; Leuchs, G. (2010): Low-Threshold Optical Parametric Oscillations in a Whispering Gallery Mode Resonator. Physical Review Letters. **105** (26): 263904.
- Ji X; Barbosa F A. S.; Roberts, S P.; Dutt, A; Cardenas, J; Okawachi, Y; Bryant, A; Gaeta, A L.; Lipson, M (2017): Ultra-low-loss on-chip resonators with sub-milliwatt parametric oscillation threshold. Optica. **4** (6): 619–624.
- Kippenberg, T. J.; Vahala, K. J. (2007): Cavity Opto-Mechanics. Optics Express. **15** (25): 17172–17205.
- Savchenkov A A.; Matsko A B.; Ilchenko, V S.; Maleki L (2007): Optical resonators with ten million finesse.
- Vahala K J. (2003): Optical microcavities. Nature. **424** (6950): 839– 846.
- Yüce E (2016): Inhibited Spontaneous Emission in Solid-State Physics and Electronics. Physical Review Letters. **78** (20): 2063–2069.